Trop J Nat Prod Res, September 2025; 9(9): 4563 - 4574 ISSN 2616-0684 (Print)
ISSN 2616-0692 (Electronic)

Tropical Journal of Natural Product Research

Available online at https://www.tjnpr.org

Original Research Article

Deciphering the protective efficacy of *Portulaca quadrifida* extract in Mitigating Cisplatin-Induced Oxidative Hepatotoxicity: Correlative *in vivo* and *in silico* analyses

Geetha Subramaniam[1]*, Helan S. Rani Michael[2], Aswini Anguraj[3], Ranjithkumar Rajamani[4], Shivakumar Bandhumy Lingam[5], Rathish Kumar Sivaraman[3*], Dinesh K.P. Bheeman[6]

[1]*Faculty of Health and Life Sciences, INTI International University, Persiaran Perdana BBN, Putra Nilai, 71800 Nilai, Negeri Sembilan, Malaysia.*
[2]*Department of Biotechnology, Manonmaniam Sundaranar University, Tirunelveli- 627 012, Tamil Nadu, India.*
[3]*Department of Biotechnology, Sri Ramakrishna College of Arts & Science, Coimbatore- 641 006, Tamil Nadu, India.*
[4]*Department of Pharmacology, Saveetha Medical College and Hospital, Saveetha Institute of Medical and Technical Sciences (SIMATS), Saveetha University, Chennai, 602105, Tamil Nadu, India.*
[5]*Department of Computer Science, Sri Ramakrishna College of Arts & Science, Coimbatore - 641 006, Tamil Nadu, India.*
[6]*Department of Applied Sciences, College of Applied Sciences and Pharmacy, University of Technology and Applied Sciences, Muscat, Sultanate of Oman.*

ARTICLE INFO

Article history:
Received 19 June 2025
Revised 05 September 2025
Accepted 06 September 2025
Published online 01 October 2025

ABSTRACT

Cisplatin (CIS) is a widely used chemotherapeutic agent, but it can cause oxidative stress-induced hepatotoxicity. In this study, *in-vivo* tests exhibited the preventive benefits of *Portulaca quadrifida* extract (PqE) against liver damage caused by cisplatin. Antioxidant activity in the liver (TBARS, GSH, GPx, SOD, CAT) and liver function tests (SGOT, SGPT, ALP, GGT) were assessed, and the ranges drastically dropped after toxic induction in the liver, as per the dosage levels. *in silico* docking studies revealed that three compounds from PqE (tetradecamethylcycloheptasiloxane, dimethyl sulfoxide, and dodecanoic acid) showed higher binding affinities towards target proteins. RMSF values were 0.24 ± 0.12 nm, 0.30 ± 0.16 nm, and 0.44 ± 0.24 nm, while the average RMSD values for the 4ZZJ-APO, 4ZZJ-DDA, and 4ZZJ-DMS were 1.03 ± 0.07 nm, 0.66 ± 0.11 nm, and 0.70 ± 0.23 nm. Additionally, dynamic stability and compactness (Rg) were demonstrated by achieving 2.34 ± 0.02 nm, 2.28 ± 0.05 nm, and 2.38 ± 0.10 nm, and SASA metrics showed 182.48 ± 4.51 nm, 181.83 ± 8.10 nm, and 189.40 ± 4.07 nm. Additionally, average intra-hydrogen bond values of 244.03 ± 8.69 nm, 245.51 ± 8.64 nm, and 243.84 ± 8.07 nm were also obtained. These results suggest that PqE protects the liver by modulating oxidative stress pathways and stabilizing key protein interactions. Overall, the study highlights the potential of PqE as a promising hepatoprotective agent for preventing cisplatin-induced liver damage.

Keywords: *Portulaca quadrifida*, Cisplatin, Hepatotoxicity, Biochemical Markers, *In-silico*, Good Health

Introduction

The liver plays a central role in the metabolism and detoxification of xenobiotics, including therapeutic agents and environmental toxins. Through a complex enzymatic system, the liver converts toxic compounds into less harmful metabolites. However, certain intermediates may remain biologically active and exert harmful effects on hepatocytes.[1,2] These metabolites can activate downstream cellular pathways that promote apoptosis, necrosis, mitochondrial dysfunction, autophagy, and dysregulated immune responses, ultimately leading to hepatocellular injury.[3,4] Cisplatin (CIS), a platinum-based Chemotherapeutic agents are widely prescribed for the treatment of multiple malignancies such as ovarian, cervical, bladder, and head-and-neck cancers.

*Corresponding author. E mail: geetha.subramaniam@newinti.edu.my
Tel: +60 12-338 8139

Citation: Subramaniam G*, Michael HSR, Anguraj A, Rajamani R, Lingam SB, Sivaraman RK*, Bheeman DKP. Deciphering the protective efficacy of *Portulaca quadrifida* extract in Mitigating Cisplatin-Induced Oxidative Hepatotoxicity: Correlative *in vivo* and *in silico* analyses. Trop J Nat Prod Res. 2025; 9(9): 4563 – 4574 https://doi.org/10.26538/tjnpr/v9i9.59

Official Journal of Natural Product Research Group, Faculty of Pharmacy, University of Benin, Benin City, Nigeria

Despite its remarkable antineoplastic efficacy, its therapeutic application is often limited by severe side effects, most notably nephrotoxicity and hepatotoxicity[5,6]. While nephrotoxicity is considered the major dose-limiting adverse effect, the mechanisms underlying CIS-induced hepatotoxicity remain insufficiently characterized. Emerging evidence suggests that oxidative stress plays a pivotal role, with CIS-induced mitochondrial dysfunction contributing to diminished membrane potential, impaired calcium regulation, and thiol depletion[7,8].

Silymarin (SIL) is a flavonoid-rich extract derived from *Silybum marianum*, which is composed of silybinin, silydianin, and silychristin. Silibinin is the primary bioactive component of SIL and exerts hepatoprotective effects through multiple mechanisms, including antioxidant activity, promotion of cell regeneration and cryoprotection. The cytoprotective effects of SIL stem from its antioxidant properties and direct interaction with cell membrane components.[9,10] The inhibition of lipid peroxidation, as demonstrated in various *in vitro* studies involving erythrocytes, isolated and cultured hepatocytes, and human mesangial cells, is recognized as one of the primary protective mechanisms of SIL. Furthermore, SIL has been shown to have antiproliferative, antifibrotic, and anti-inflammatory properties.[11,12] Numerous biochemical processes occur within the cell, such as the activation of polymerase I rRNA transcription, which stimulates the production of ribosomal RNA (rRNA).[13-15] These reactions also protect against cell damage caused by free radicals and prevent the absorption of toxins, contributing to the protective potential of SIL.[16,17] SIL helps

prevent liver enlargement by inhibiting 5-lipoxygenase, reducing leukotriene production, and limiting free radical generation in Kupffer cells.[18] Additionally, silybin has been shown to protect hepatocytes from membrane lipid peroxidation and cellular damage. Various animal studies have shown that silymarin effectively counteracts drug-induced hepatotoxicity. Its hepatoprotective effects are attributed primarily to its potent antioxidant activity, which promotes cell regeneration and cytoprotective effects.[19, 20] Plants with strong ethnomedical backgrounds play a crucial roles in preventive medicine and in the management of diverse human ailments.[21,22] Studies have highlighted the therapeutic potential of natural products, particularly polyphenolic compounds, in combating organ pathologies caused by oxidative stress.[23,24] Compared with synthetic antioxidants, plant-derived compounds are generally considered safer and often provide broader biological benefits. Plant-based products are important sources for development of effective medications and also play a crucial role in enhancing human health and wellness.[25,26,27] *Portulaca quadrifida* (Pq), commonly known as chicken weed, is a small, prostrate, perennial herb in the Portulacaceae family. It is widely distributed across Asia and Africa and has been extensively used in traditional medicine for centuries. Traditional practices show that Pq has been used to treat various health issues, such as asthma, inflammation, hemorrhoids, gastric ulcers, erysipelas, abdominal problems, eye inflammation, and urinary problems.[28]

Modern pharmacological research indicates that Pq has a broad spectrum of biological activities, including antimicrobial, anticancer, antihyperglycemic, antioxidant[29], neuropharmacological[30], antifungal activity against *Candida albicans* and *Aspergillus fumigatus*[31], and wound healing properties.[32] Phytochemical analysis of the ethanolic extract of Pq revealed flavonoids and alkaloids, which are believed to contribute to its therapeutic effects.[33] These findings prompted us to investigate the hepatoprotective effects of Pq against chemotherapeutic agents such as CIS. To our knowledge, the in vivo toxicological and nephroprotective effects of PqE have not been reported. In the present study, we explored novel approaches to reduce the toxic effects of CIS on liver biochemical markers in Swiss albino mice, and antioxidant activity was evaluated via *in silico* studies.

Materials and Methods

Plant collection and extract preparation

The study involved the collection of fresh *Portulaca quadrifida* leaves from Sathyamangalam, Tamil Nadu, India (11°30'17.1936"N and 77°14'18.2256"). The leaves were washed with tap water, followed by distilled water to remove dust. They were also kept dry in a shaded area for ten days. A mill and pestle were subsequently used to grind the leaves into a fine powder. After 10 g of leaf powder was dissolved in 100 mL of distilled water, the PqE was incubated for 24 hours at 37°C. The extracts were dried via a rotary evaporator set at 45°C and stored until use. All chemicals and reagents were of analytical or reagent grade from Sigma Aldrich (Massachusetts, USA).

Gas Chromatography-Mass Spectrometry (GC-MS)

The aqueous extract was analyzed through GC-MS analysis by the Indian Institute of Technology, Mumbai. The analysis was carried out on a THERMO MS DSQ II system equipped with a standard nonpolar DB 35-MS capillary column. Helium served as the carrier gas during the run. The injector temperature was initially set at 70 °C and was gradually increased to 260 °C at a programmed rate of 6 °C per minute. The total runtime for the sample was 30 minutes and 51 seconds.

Animal Experiments

Twenty-five male albino mice aged two weeks and free of pathogens were collected from Venkateswara Enterprises, Bangalore. The Institutional Animal Ethics Committee approved the study (Reg. No. IAEC/KASC/MSC/013/20017-14) as described by Chen et al.[34] After an acclimation period, the animals were randomly assigned into five groups of five mice each. The dosing regimen was adapted with minor modifications from the method described by Chen et al.[34] Standard laboratory conditions, including a temperature of 24 °C, relative humidity of 30-70%, and a 12-hour light/dark cycle, were maintained throughout the study. All animals were provided a standard chow diet and subjected to a minimum fasting period of 12 hours before experimentation.

Inclusion Criteria

Animal species: Swiss albino mice
Gender: The document does not specify the gender of the mice, so it can be assumed that both male and female mice were included
Age & weight range: The document does not provide details on the age or weight range of the mice used in the study.
Health status: The mice were healthy and not previously exposed to experimental treatments or procedures.
Induction of cisplatin-induced hepatotoxicity: The mice were administered cisplatin to induce liver damage and toxicity.

Treatment groups

In the Control group (Group I): 1 mL of normal saline was administered orally for 20 consecutive days (0.9 g NaCl in 100 mL H_2O).
PqE group (Group II): Mice received the aqueous extract of *Portulaca quadrifida* 200 mg/kg, oral) for 15 days.
In the Cisplatin (CIS) group (Group III): Mice received cisplatin (3.5 mg/kg) in normal saline through the i.p. for 5 days.
CIS + PqE group (Group-IV): Mice received Cisplatin (3.5 mg/kg) in normal saline through i.p. route for 5 days after being treated with 10% ethanolic extract of *P. quadrifida* (200 mg/kg, oral) for 15 days.
CIS + SIL group (Group-V): Mice were administered cisplatin (3.5 mg/kg) in normal saline *via* intraperitoneal injection for 5 days, followed by treatment with silymarin (50 mg/kg orally).
The inclusion criteria ensured that the researchers had a consistent and appropriate animal model to investigate the protective effects of *P. quadrifida* extract and silymarin against cisplatin-induced hepatotoxicity.

Exclusion Criteria

To confirm that the observed hepatotoxic effects were caused by cisplatin treatment, we excluded mice with pre-existing liver damage or unrelated diseases. Additionally, mice showing significant health issues or abnormalities beyond cisplatin toxicity would be removed to maintain the study's integrity and prevent confounding effects. Mice that had previously received experimental therapies, such as silymarin or Pq extract, were also excluded to avoid potential side effects.

Experimental Design

After treatment, all the mice were anesthetized with diethyl ether, and the thoracic and abdominal cavities were opened along the midline. The liver was meticulously dissected, ensuring that it was removed from the surrounding connective tissue and fat. The tissue was then prepared for further analysis by being rinsed with molecular saline, blotted with filter paper, and finally washed with ice-cold saline.

Determination of biochemical parameters and histopathological analysis

The levels of SGOT, SGPT[35], ALP, and GGT[36] were analyzed. The livers were preserved in 10% neutral buffered formalin for 24 hours. Before use, the plant materials were sanitized with 70% ethanol. The tissues were subsequently mixed in a small metal container via a magnetic stirrer. The tissues were also dehydrated with various alcohol solutions, ranging from 70% to 100%, to eliminate moisture. The paraffin blocks were subsequently sectioned with a rotary ultramicrotome, placed onto glass slides, and allowed to dry overnight after the tissues had been soaked. The slides were mounted, stained with hematoxylin and eosin (H&E), and examined with a light microscope (Nikon Eclipse E200, Nikon Corporation, Japan).

Antioxidant assays

After adding 1.2 mL of PBS to a 20 mg liver sample, the samples were ground using a mortar and pestle. Following transfer into a new centrifuge tube, the homogenized tissues were centrifuged for 10 minutes at 4°C at 12,000 rpm. For the estimation of TBARS[37], GSH[38], CAT[39], SOD[40], and GPx[41], the supernatant was collected.

ISSN 2616-0684 (Print)
ISSN 2616-0692 (Electronic)

In silico studies

In silico analysis was performed using compounds identified through GC-MS profiling. The 2D structures of the detected molecules were retrieved from PubChem and evaluated for their predicted biological activities via the PASS server. To investigate hepatotoxicity, the liver metabolic pathway was examined to identify proteins associated with liver injury, and their corresponding 3D structures were obtained from the Protein Data Bank (PDB). The protein structures were visualized and refined via Discovery Studio Visualizer, which facilitated the identification of active binding sites. Molecular docking studies were then carried out via ArgusLab, and the drug-likeness and efficacy of the compounds were further assessed with Lead[42]

Ligand molecule preparation

The structures of the three Pq compounds, including dimethyl sulfoxide, tetradecamethylcycloheptasiloxane, and dodecanoic acid 1, 2, 3-propanetriyl ester, were obtained from the NCBI PubChem Compound database. These ligands were optimized via Discovery Studio Visualizer (DSV) v21.1.0.20298, a product from BIOVIA, a company based in San Diego, CA, USA, which belongs to Dassault Systèmes. Energy minimization was conducted to resolve atomic collisions within the ligands, ensuring their stability. This process utilized the CHARMm (Chemistry at HARvard Macromolecular Mechanics) force field, which is a part of Discovery Studio. Various conformations of the ligands were generated and assessed based on bond energy, CHARMm energy, dihedral energy, electrostatic energy, initial potential energy, and the RMS gradient [43,44,45]

Molecular docking

Molecular docking simulations at pH 7.4 were performed in the present work via AutoDock Vina through the AMDock platform, and focusing the search on the heteroatoms of the target receptor while considering ionization states critical for binding. Simulations at physiological pH ensured the accurate prediction of ligand-receptor interactions. Hypothesized binding positions and specificities in the receptor's active site were identified through an effective ligand conformation search facilitated by the adopted methodology.

Molecular dynamics

After analyzing the crystal structure of the SIRT1/activator/substrate complex (4ZZJ), we conducted docking analysis to identify the top two ligands: 4ZZJ-DDA and 4ZZJDMS. To parameterize the ligands, including generating their topology, we utilized the ATB server. The GROMACS pdb2gmx module was employed to incorporate hydrogen atoms into the heavy atoms. The systems were equilibrated for 1500 steps under low vacuum energy using the steepest descent method. The structures were subsequently solvated in a cubic periodic box with a simple point charge (SPCE) water model. Sodium and chloride counterions were added to achieve a salt concentration of 0.15 M. The system setup was based on a previously published study (PMID: 31514687).[46,47] The final structures from the NPT equilibration stage served as the starting configurations for NPT production runs; each structure was simulated for 200 ns. GROMACS software was used to evaluate the simulation trajectory in various ways, including protein RMSD, RMSF, RG, SASA, and H-bond analysis. Throughout the molecular dynamics (MD) simulation, the Molecular Mechanics Poisson-Boltzmann Surface Area (MM-PBSA) method was utilized to determine the binding free energy between the protein and the inhibitors 4ZZJ-DDA and 4ZZJ-DMS. The binding free energy for the last 50 ns of the receptor's active site was computed via the GROMACS tool at intervals of 1000 frames.

Results and Discussion

Gas Chromatography-Mass Spectrometry

GC-MS analysis of the ethanolic extract of PqE identified eight phytochemicals. Among these, dimethyl sulfoxide (RT: 3.34 min), tetradecamethylcycloheptasiloxane (RT: 13.54 min), and dodecanoic acid 1,2,3-propanetriyl ester (RT: 26.66 min) were the predominant constituents and presented the highest peak intensities (Figure 1). The presence of these bioactive compounds may contribute to the antioxidant and hepatoprotective potential of PqE. Dimethyl sulfoxide is a well-known free radical scavenger with membrane-stabilizing properties, while fatty acid esters such as dodecanoic acid derivatives have been reported to exhibit antioxidant, anti-inflammatory, and cytoprotective effects. Similarly, siloxane derivatives, although often considered artifacts, have been associated with protective biological activities in some studies. These findings suggest that the phytoconstituents of PqE may act synergistically to mitigate oxidative stress and support liver function, which is consistent with the biochemical and histological outcomes observed in cisplatin-treated mice[29].

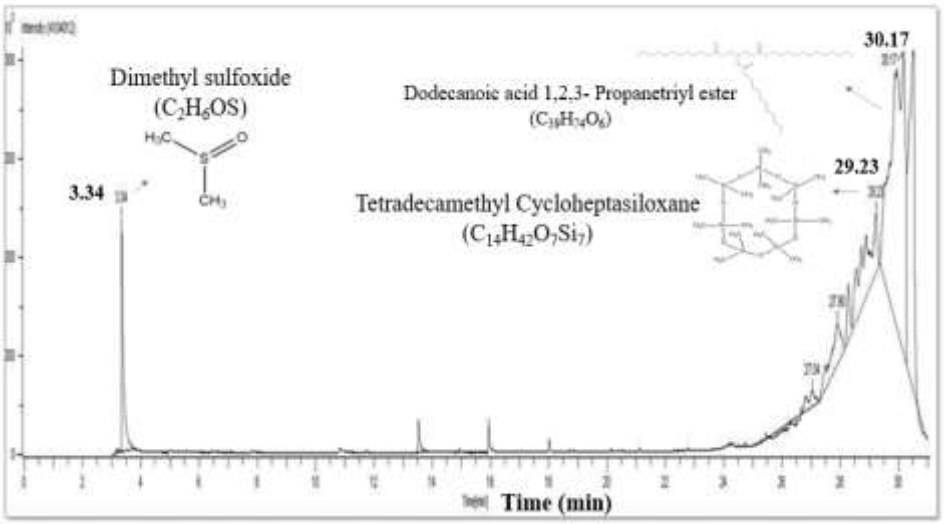

Figure 1: GC-MS analysis of *Portulaca quadrifida* extract (PqE)

Assessment of hepatotoxicity

Determination of biochemical parameters

In cases of severe liver damage, cytoplasmic enzymes such as SGOT, SGPT, ALP, and GGT leak into the bloodstream. These enzymes are commonly used as indicators of liver diseases and myocardial infarctions. In the present study, serum samples from control and treated mice were analysed, which revealed a significant increase in hepatic marker enzyme levels following cisplatin administration. Specifically,

ISSN 2616-0684 (Print)
ISSN 2616-0692 (Electronic)

SGOT increased from 56 ± 1.54 U/L to 91 ± 1.19 U/L, SGPT from 73 ± 0.60 U/L to 109 ± 2.62 U/L, ALP from 110 ± 0.65 U/L to 184 ± 5.14 U/L, and γ-GT from 40 ± 1.06 U/L to 83 ± 1.88 U/L (Figure 2). These findings confirm that CIS-induced hepatotoxicity results in leakage of hepatic enzymes into circulation. Oral administration of PqE (200 mg/kg b.w) and silymarin (50 mg/kg b.w) significantly reduced the elevated enzyme levels, restoring them nearly to normal. Therefore, demonstrating the hepatoprotective effect of PqE is comparable to that of the standard drug silymarin. The protective effect of PqE may be attributed to its high content of flavonoids and alkaloids, which are reported to have anti-inflammatory, antithrombotic, hepatoprotective, and anticancer properties. Extracts of *P. odoratissimus* containing 0.50% (w/w) total flavonoids and 11.62% (w/w) total phenolics have shown potent antioxidant activity with an IC_{50} value < 31.25 ppm. These phytoconstituents are known to stabilize hepatocyte membranes, prevent the leakage of SGOT, SGPT, ALP, and γ-GT, and control bilirubin levels in serum. Moreover, oleracone, the first alkaloid identified in *P. oleracea*, has demonstrated anti-inflammatory activity in lipopolysaccharide-stimulated macrophages. It enhances T-lymphocyte and NK cell responses, while modulating inflammatory cytokines (IL-4, IL-10, IFN-γ, and TNF-α), thereby reducing inflammation and maintaining immune homeostasis through regulation of the Th1/Th2 balance. These immunomodulatory and antioxidant properties likely contribute to the observed hepatoprotective effects of PqE[48].

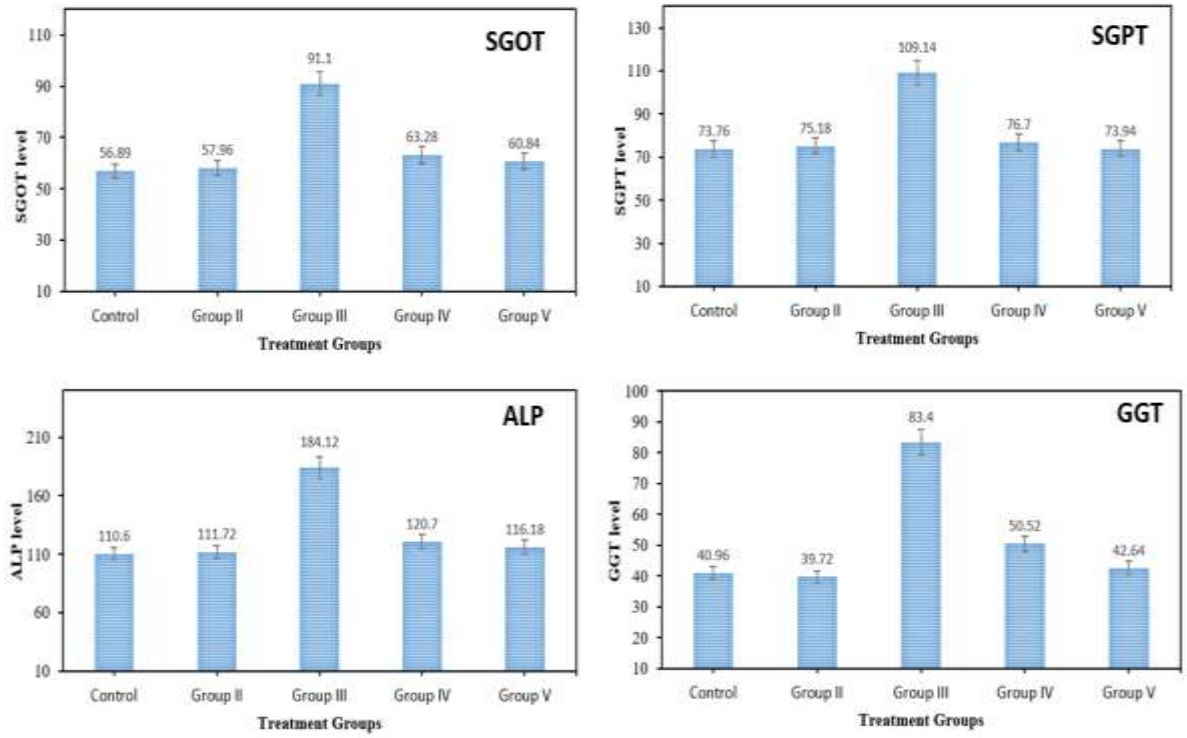

Figure 2: Effects of PqE on serum (SGOT, SGPT, ALP, and GGT levels) and CP-induced hepatotoxicity

Histopathological analysis

The histopathological findings further supported the biochemical results (Figure 3). Liver sections from the CIS-treated group showed severe pathological changes, including hepatocyte degeneration, necrosis, and dense perivascular lymphocytic infiltration, confirming CIS-induced hepatotoxicity. In contrast, mice treated with PqE (200 mg/kg b.w) and SIL (50 mg/kg b.w) maintained normal hepatocytes with minimal perivascular inflammatory infiltration. These observations align with the biochemical data, further highlighting the protective role of PqE against CIS-induced liver injury. Research has indicated that *Portulaca oleracea* L., a closely related species, exhibits potent hepatoprotective effects in experimental models of liver injury caused by agents such as carbon tetrachloride, cisplatin, acetaminophen, and high-fat diets. Its bioactive compounds have been shown to decrease oxidative stress, inhibit inflammation, and slow the development of hepatocellular carcinoma and hepatic fibrosis. Moreover, control mice presented normal liver histology, whereas untreated CIS mice presented extensive perivascular lymphocytic infiltration and structural disorganization. Treatment with PqE and silymarin helped restore liver tissues toward normal levels, highlighting their potential as natural agents for liver protection.

Antioxidant studies

Oral administration of PqE significantly restored antioxidant levels in CIS-induced mice and ameliorated cisplatin-mediated hepatic alterations. The liver relies on both enzymatic and non-enzymatic antioxidants to combat reactive oxygen species (ROS)-induced oxidative stress. Among these, glutathione (GSH), a major intracellular non-protein thiol, plays a pivotal role in detoxification, while catalase (CAT) and glutathione peroxidase (GPx) neutralize hydrogen peroxide, and superoxide dismutase (SOD) catalyzes the dismutation of superoxide radicals into less reactive species. In CIS-treated mice, the GSH level decreased significantly from 7.85 ± 0.64 to 4.20 ± 0.42 mg/g tissue, the GPx activity decreased from 35.14 ± 2.51 to 23.19 ± 1.62 µmol NADPH oxidized/mg protein/min, SOD activity from 13.88 ± 1.01 to 7.62 ± 0.23 U/mg protein/min, and the CAT activity decreased from 63.92 ± 4.94 to 38.24 ± 1.15 µmol H_2O_2/mg protein/min. (Figure 4). These improvements highlight the strong antioxidant potential of PqE, likely because its bioactive constituents are capable of scavenging free radicals and reinforcing endogenous defense mechanisms. Comparable protective effects of *Portulaca oleracea* against cisplatin-induced oxidative damage have also been demonstrated by Sudhakar et al. (2010)[51].

ISSN 2616-0684 (Print)
ISSN 2616-0692 (Electronic)

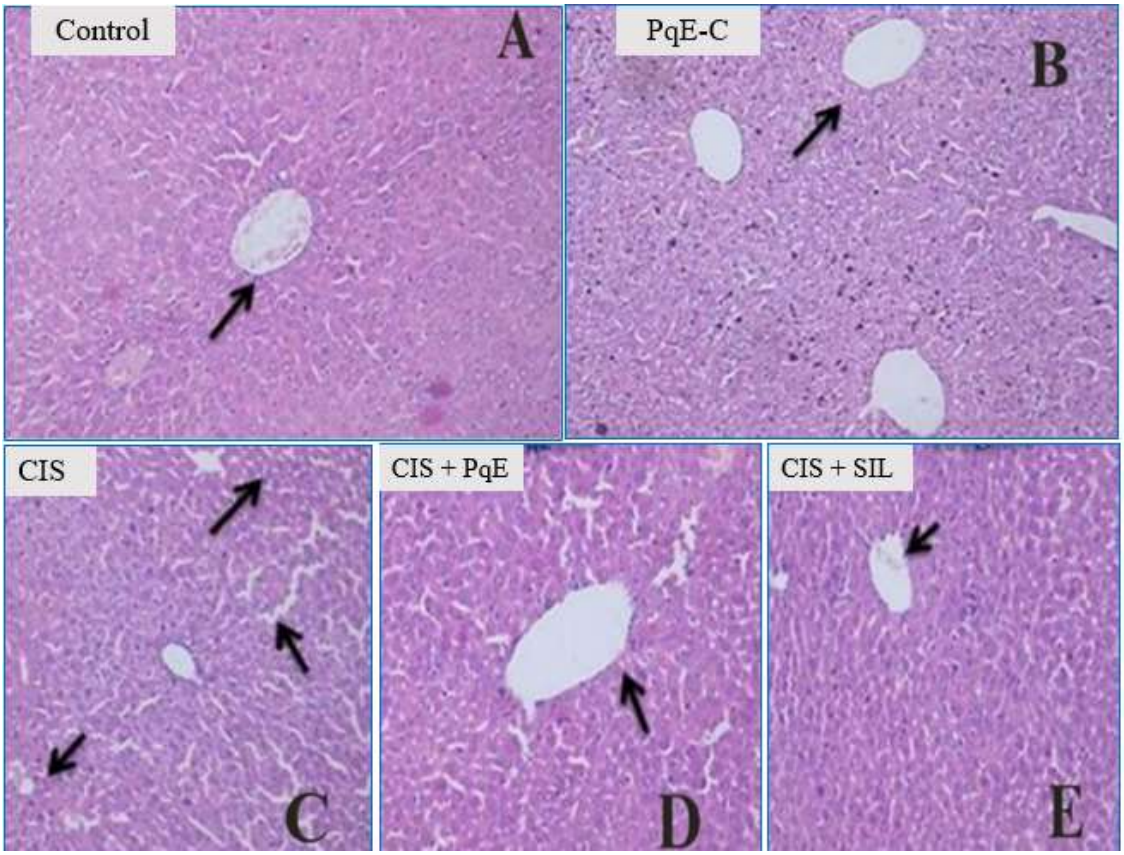

Figure 3: Histopathological analysis A) Control, B) PqE-C, C) CIS, D) CIS + PqE, and E) CIS + SIL groups

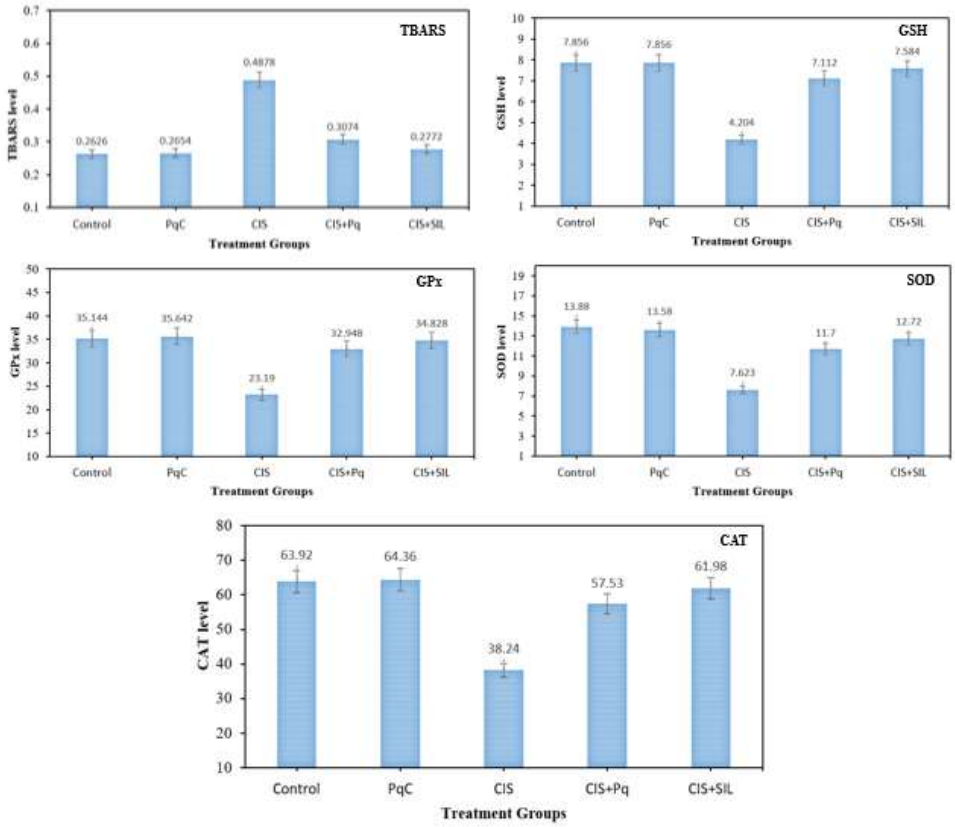

Figure 4: Effects of PqE on MDA levels and liver antioxidant activity in patients with CP-induced nephrotoxicity (TBARS, GSH, GPx, SOD, and CAT)

ISSN 2616-0684 (Print)
ISSN 2616-0692 (Electronic)

In-silico studies

Molecular Docking

Molecular docking was carried out via the predicted protein model with AutoDock Vina integrated in AMDock. The binding affinities of the selected ligands with the target proteins are summarized in Table 1, and their corresponding 2D interaction profiles are illustrated in Figure 5.

Molecular Dynamics

All-atom MD simulations were performed to evaluate the structural stability and conformational dynamics of the protein–ligand complexes. Compared with the 4ZZJ–DDA complex, the 4ZZJ–DMS complex presented lower RMSD values and reduced active-site flexibility, suggesting enhanced stability. The Rg values remained stable, with DDA showing a slight reduction, indicating improved compactness. SASA revealed decreased solvent exposure in the DDA complex, further supporting tighter binding. The hydrogen bonding profiles revealed that DDA maintained more persistent interactions than did DMS throughout the trajectory, which is in agreement with the MMPBSA findings. Together, these results demonstrate that DDA forms a stable and compact complex with the target protein, which may underlie its hepatoprotective potential. Similar approaches have highlighted the utility of MD simulations in validating docking predictions and understanding ligand-induced stability[52, 53].

Table 1: Protein interactions and the docking scores

Protein-Ligand Complex	Docking score	Interactions
4ZZJ-DDA	-8.9	SER441, SER442, LEU443, ALA262, PHE273, PHE312, ILE316, ILE347
4ZZJ-DMS	-8.8	SER442

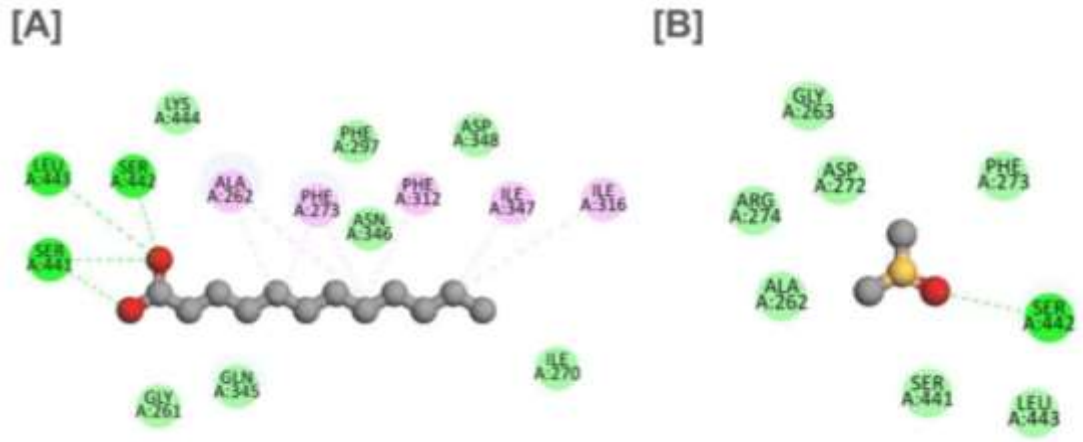

Figure 5: 2D images of the protein-ligand interactions of (A) 4ZZJ-DDA and (B) 4ZZJ-DMS complexes.

Root Mean Square Deviation (RMSD)

RMSD analysis was performed to evaluate the conformational stability of the protein–ligand complexes. Both systems reached equilibrium within 5 ns and maintained stability throughout the 100 ns simulation. The average RMSD values were 1.03 ± 0.07 nm for 4ZZJ-APO, 0.66 ± 0.11 nm for 4ZZJ-DDA, and 0.70 ± 0.23 nm for 4ZZJ-DMS, indicating that the ligand-bound complexes displayed reduced fluctuations compared with the apo form, confirming stable binding (Figure 6). These findings suggest that the presence of ligands enhances the structural stability of the protein, as complexes with RMSD values below 0.3–0.5 nm are generally considered stable interactions in MD simulations. The lower RMSD fluctuations of 4ZZJ-DDA and 4ZZJ-DMS relative to 4ZZJ-APO highlight their potential as effective binders that stabilize the protein structure[52, 53].

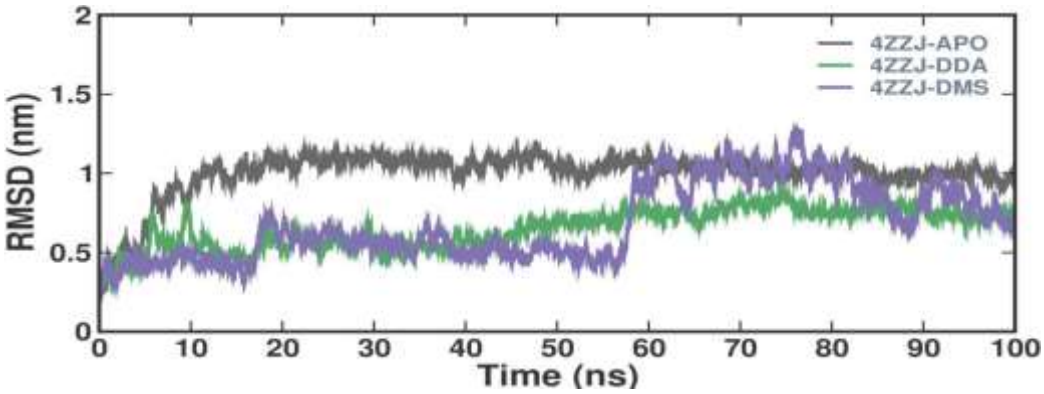

Figure 6: RMSD Conformational dynamics analysis of 4ZZJ-APO, 4ZZJ-DDA, and 4ZZJ-DMS

ISSN 2616-0684 (Print)
ISSN 2616-0692 (Electronic)

Root Mean Square Fluctuation (RMSF)

Root Mean Square Fluctuation (RMSF) was employed to evaluate the flexibility of residues and identify regions susceptible to conformational changes within the protein-ligand complexes. The mean RMSF values calculated for the 4ZZJ-APO, 4ZZJ-DDA, and 4ZZJ-DMS complexes were 0.24 ± 0.12 nm, 0.30 ± 0.16 nm, and 0.44 ± 0.24 nm, respectively. As expected, rigid structural domains such as helices and β-sheets presented lower RMSF values, whereas loop regions presented comparatively greater fluctuations. The results suggest that ligand binding did not cause significant structural deviations, and both 4ZZJ-DDA and 4ZZJ-DMS maintained stable dynamic profiles throughout the simulation (Figure 7). Notably, 4ZZJ-DDA exhibited lower fluctuations than did 4ZZJ-DMS, implying that DDA binding imparts additional rigidity to the protein, which may have contributed to the higher binding affinity observed in MMPBSA analysis. These findings are consistent with earlier reports indicating that ligand binding often stabilizes key structural elements of proteins while permitting flexibility in the loop[52].

Radius of gyration (Rg)

The radius of gyration (Rg) was analyzed to evaluate the structural compactness and dynamic stability of the protein-ligand complexes during the simulation. The mean Rg values were 2.34 ± 0.02 nm for 4ZZJ-APO, 2.28 ± 0.05 nm for 4ZZJ-DDA, and 2.38 ± 0.10 nm for 4ZZJ-DMS (Figure 8). The comparable Rg values observed across all the complexes suggest that ligand binding did not induce major structural rearrangements, and that both 4ZZJ-DDA and 4ZZJ-DMS maintained compactness throughout the trajectory. The slightly reduced Rg in the 4ZZJ-DDA complex implies marginally enhanced stability compared with that of APO and DMS systems. These findings are consistent with earlier studies showing that stable Rg values indicate a balanced distribution of protein mass and minimal conformational drift during molecular dynamics simulations[53]. To complement the Rg analysis, the solvent accessible surface area (SASA) was calculated to assess changes in protein exposure to the solvent environment upon ligand binding. The mean SASA values were 182.48 ± 4.51 nm² for 4ZZJ-APO, 181.83 ± 8.10 nm² for 4ZZJ-DDA, and 189.40 ± 4.07 nm² for 4ZZJ-DMS (Figure 9). The stable SASA profiles indicate that ligand binding did not significantly alter solvent exposure, although 4ZZJ-DMS showed marginally higher values, reflecting localized flexibility. Together, the results of the Rg and SASA analyses confirmed that both complexes remained stable, with 4ZZJ-DDA exhibiting slightly greater compactness and structural stability.

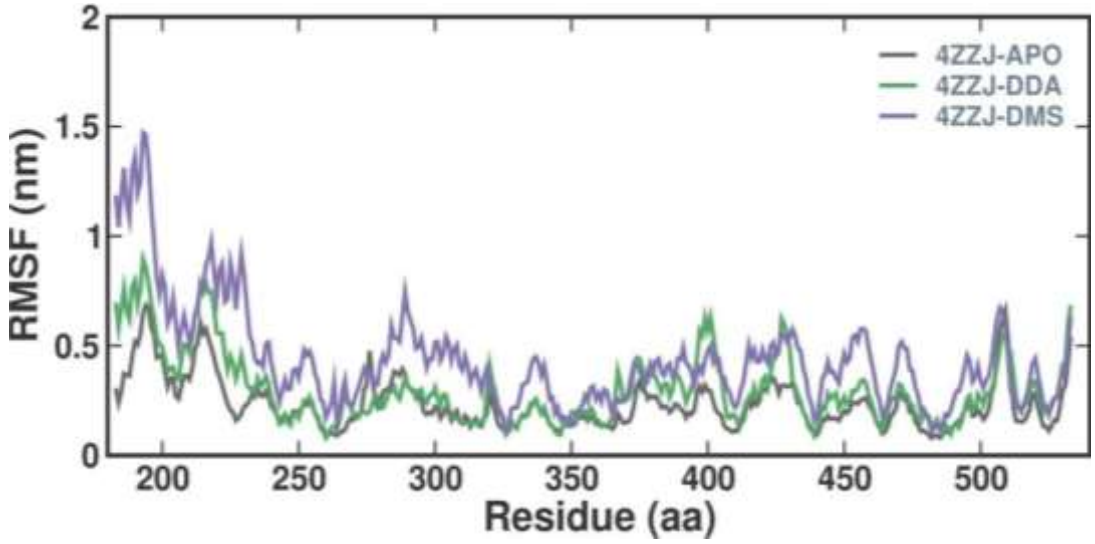

Figure 7: Conformational dynamics analysis of the 4ZZJ-APO, 4ZZJ-DDA, and 4ZZJ-DMS complexes *via* RMSF

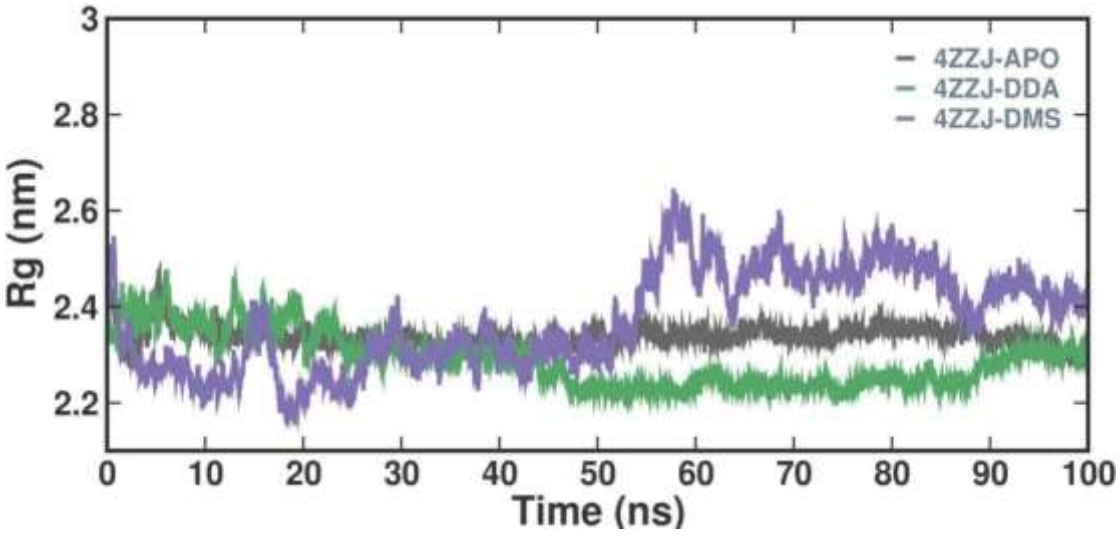

Figure 8: Conformational dynamics analysis of the 4ZZJ-APO, 4ZZJ-DDA, and 4ZZJ-DMS complexes *via* Rg

ISSN 2616-0684 (Print)
ISSN 2616-0692 (Electronic)

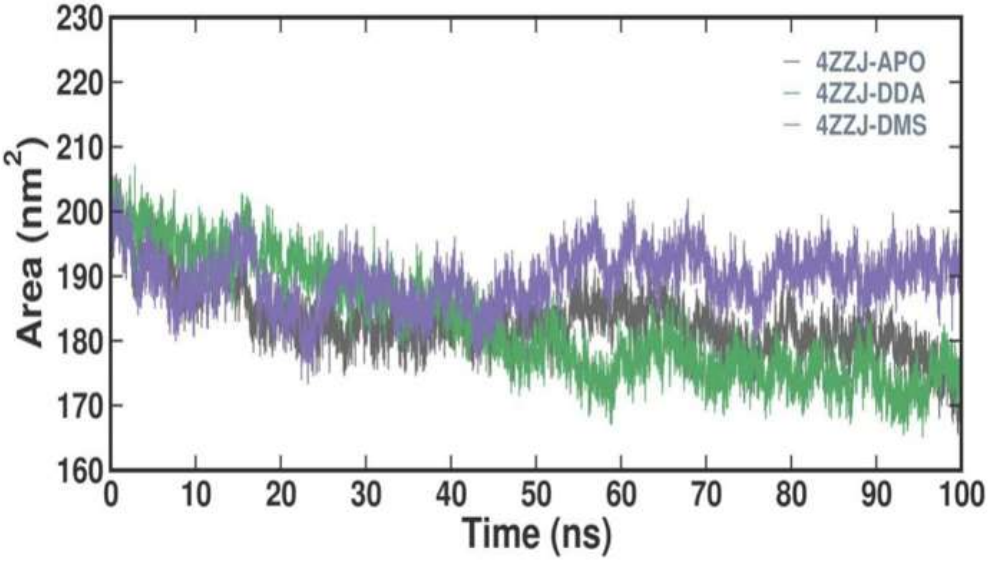

Figure 9: Conformational dynamics analysis of the 4ZZJ-APO, 4ZZJ-DDA, and 4ZZJ-DMS complexes *via* SASA

Inter and intra-hydrogen bonds

Hydrogen bonding analysis was carried out to evaluate the stability of the unbound protein (4ZZJ-APO) and the protein-ligand complexes (4ZZJ-DDA and 4ZZJ-DMS). The average number of intra-hydrogen bonds was found to be 244.03 ± 8.69, 245.51 ± 8.64, and 243.84 ± 8.07 for 4ZZJ-APO, 4ZZJ-DDA, and 4ZZJ-DMS, respectively. The slightly greater number of hydrogen bonds in the ligand-bound systems than in the unbound protein suggests that ligand interactions contribute to maintaining structural integrity (Figure 10). Hydrogen bonds also play a central role in stabilizing protein–ligand interactions. The 4ZZJ-DMS complex consistently maintained 1–2 hydrogen bonds, while the 4ZZJ-DDA complex displayed 1-6 hydrogen bonds throughout the simulation (Figure 11). These stable hydrogen bonding patterns indicate persistent and favorable contacts between the ligands and the target protein, which contribute to overall conformational stability. The hydrogen bond dynamics observed in this study align with earlier reports that emphasize the role of stable hydrogen bond networks in maintaining intramolecular structure and stabilizing protein–ligand interactions during molecular dynamics simulations[54,55]. These findings indicate that both DDA and DMS contribute to the structural stability of the target protein, with DDA exhibiting more dynamic and variable hydrogen bonding interactions than DMS does.

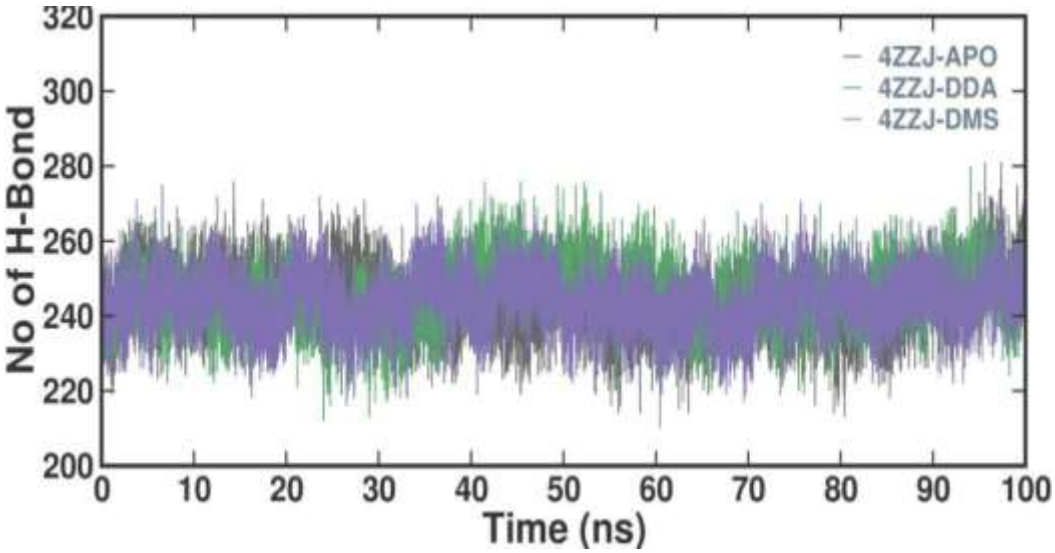

Figure 10: Intramolecular hydrogen bonds 4ZZJ-APO, 4ZZJ-DDA, and 4ZZJ-DMS during the simulation time

Principal component analysis (PCA)

The collective motions of the 4ZZJ-APO, 4ZZJ-DDA, and 4ZZJ-DMS complexes were investigated via principal component analysis (PCA). The first few eigenvectors (EVs) captured the essential motions of the systems, providing insights into their conformational dynamics. The PCA trajectories revealed that the overall flexibility of the protein decreased upon ligand binding, as both the 4ZZJ-DDA and 4ZZJ-DMS complexes showed reduced large-scale fluctuations compared with the APO form (Figure 12). The conformational space occupied by the three systems overlapped extensively, indicating that ligand binding did not introduce significant structural deviations. These results suggest that DDA and DMS binding conferred stability to the protein by restricting conformational variability. Such stabilization is consistent with earlier findings where ligand interactions were shown to limit the accessible conformational space of proteins, thereby increasing their structural resilience[53]. Overall, the PCA results highlight that both ligands stabilize the target protein without imposing conformational strain, supporting their potential role as effective stabilizers.

ISSN 2616-0684 (Print)
ISSN 2616-0692 (Electronic)

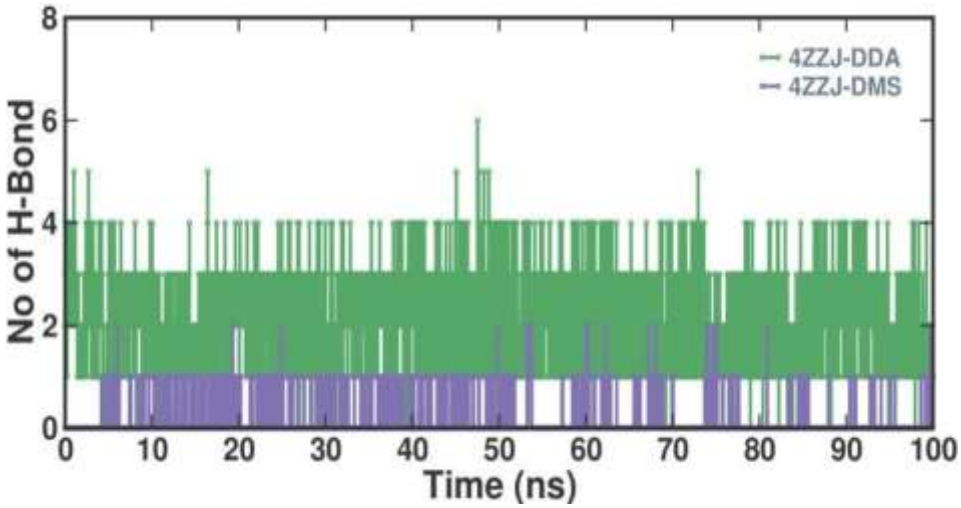

Figure 11: Intermolecular H-bond interactions between protein-ligand during the simulation time

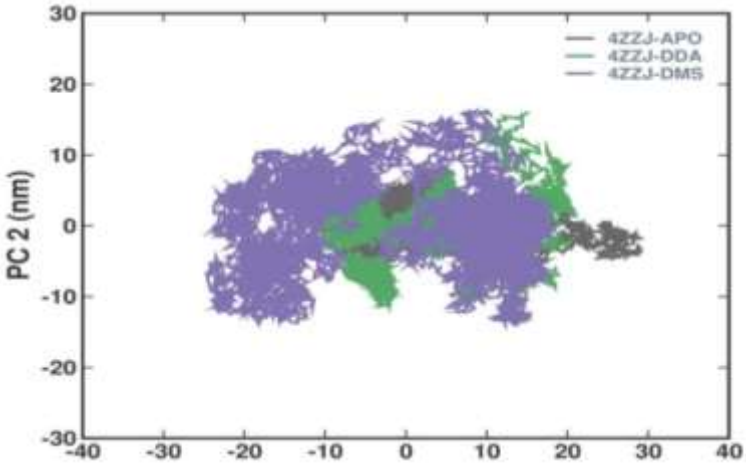

Figure 12: 2D projection plot for 4ZZJ-APO, 4ZZJ-DDA, and 4ZZJ-DMS confirmation samples

Free Energy Landscapes (FELs)

The free energy landscape (FEL) method is a popular approach for studying protein folding pathways and stability during molecular dynamics simulations. FEL plots help identify stable conformations by showing the free energy minima of the system. In this study, FELs were created for the first two principal components (PC1 and PC2) of the protein-ligand complexes (Figure 13). The results revealed that the free energy ranged from 0 to 14 kJ/mol for the 4ZZJ-DMS complex and from 0 to 16 kJ/mol for the 4ZZJ-APO and 4ZZJ-DDA complexes. The FEL plots indicated that both 4ZZJ-DDA and 4ZZJ-DMS occupied broad, deep energy basins with a single global minimum, suggesting that these ligands stabilize the target protein without causing major conformational changes. The dominance of low-energy basins in the docked complexes, compared with the APO form, suggests increased conformational rigidity and improved thermodynamic stability of the protein-ligand complexes. These results align with previous studies that show that stable FEL basins are signs of ligand-induced stabilization of protein structures[54].

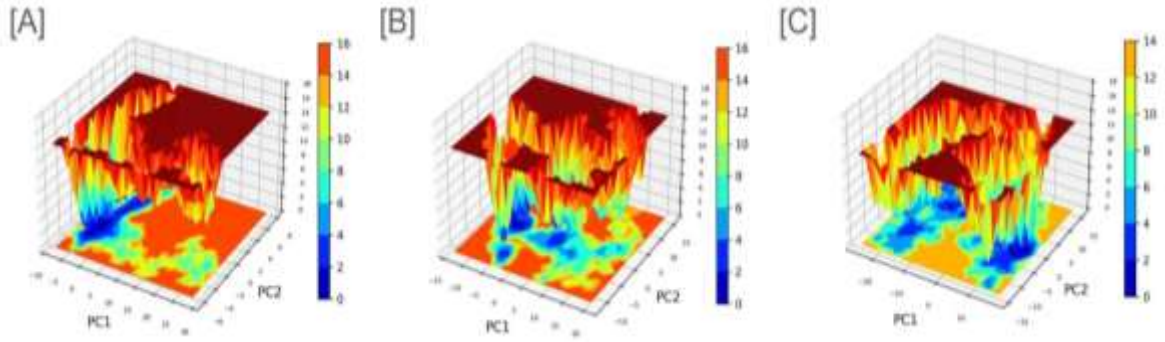

Figure 13: Free energy landscape plots: (A) 4ZZJ-APO, (B) 4ZZJ-DDA, (C) 4ZZJ-DMS complexes.

MM -PBSA

The binding free energy of the protein-ligand complexes was calculated via the MM-PBSA approach to evaluate the interaction stability of 4ZZJ-DDA and 4ZZJ-DMS. Table 2 reveals that the 4ZZJ-DDA complex displayed a substantially stronger binding affinity than did 4ZZJ-DMS. Specifically, 4ZZJ-DDA exhibited a polar solvation energy of 123.379 ± 25.215 kJ/mol, an electrostatic energy of -55.569 ± 20.502 kJ/mol, a van der Waals contribution of -94.942 ± 11.243 kJ/mol, and an overall binding free energy of -42.375 ± 4.304 kJ/mol. In contrast, 4ZZJ-DMS showed relatively weaker interactions, with van der Waals, electrostatic, and polar solvation energies of -23.812 ± 11.168 kJ/mol, -16.151 ± 8.553 kJ/mol, and 30.380 ± 17.683 kJ/mol, respectively, resulting in a much less favorable binding energy of -13.591 ± 10.031 kJ/mol. These results suggest that van der Waals and electrostatic contributions were the major stabilizing forces in the 4ZZJ-DDA complex, leading to its higher affinity, whereas unfavorable polar solvation energies in 4ZZJ-DMS weakened its binding. These findings are consistent with previous reports indicating that van der Waals and electrostatic interactions often dominate in protein-ligand binding stability[55,56]. Overall, the MM-PBSA analysis results support the superior binding strength of 4ZZJ-DDA over 4ZZJ-DMS, reinforcing its potential as a more effective ligand candidate.

Table 2: Comparison of the inhibitory binding strengths of 4ZZJ-DDA and 4ZZJ-DMS

System	Van der Waals energy	Electrostatic energy	Polar solvation energy	Binding energy
4ZZJ-DDA	-94.942 +/- 11.243 kJ/mol	-55.569 +/- 20.502 kJ/mol	123.379 +/- 25.215 kJ/mol	-42.375 +/- 4.304 kJ/mol
4ZZJ-DMS	-23.812 +/- 11.168 kJ/mol	-16.151 +/- 8.553 kJ/mol	30.380 +/- 17.683 kJ/mol	-13.591 +/- 10.031 kJ/mol

Conclusion

The present study demonstrated that *Portulaca q uadrifida* extract (PqE) exerts significant hepatoprotective effects against cisplatin (CIS)-induced toxicity. GC–MS analysis confirmed the presence of eight phytoconstituents, among which dimethyl sulfoxide, tetradecamethylcycloheptasiloxane, and dodecanoic acid 1,2,3-propanetriyl ester were predominant. These bioactive compounds are likely responsible for the observed antioxidant, anti-inflammatory, and cytoprotective effects. Biochemical evaluations revealed that PqE administration effectively normalized the levels of serum hepatic enzyme markers (SGOT, SGPT, ALP, and γ-GT), which were elevated due to CIS treatment. Furthermore, PqE significantly restored glutathione (GSH) levels and improved the antioxidant defense system, thereby counteracting oxidative stress. Histopathological observations supported these biochemical findings, showing preserved hepatocyte morphology and minimal perivascular inflammatory infiltration in the PqE-treated groups compared with the severe liver injury observed in CIS-only animals. These findings indicate that PqE mitigates CIS-induced hepatotoxicity through a multifaceted mechanism involving the modulation of oxidative stress, enhancement of endogenous antioxidant defenses, and protection of liver architecture. The results highlight the potential of PqE as a natural, cost-effective adjuvant therapy during cisplatin chemotherapy to reduce hepatotoxic side effects and improve patient outcomes. Future studies, including clinical validations and mechanistic explorations at the molecular level, are warranted to fully establish its therapeutic applicability.

Conflict of interest

The author`s declare no conflicts of interest.

Authors' Declaration

The authors hereby declare that the work presented in this article is original and that any liability for claims relating to the content of this article will be borne by them.

Acknowledgements

This study was conducted under the principles outlined in the declaration, and approval was granted (Reg. No. IAEC/KASC/MSC/013/20017-14) by the Institutional Animal Ethics Committee members of Kongunadu Arts and Science College, Coimbatore. (Dr. Hariharan, Veterinarian, Dr. Ariharasivakumar, Professor, Pharmacology Department, KMCH college of pharmacy, Coimbatore & Dr. C. Gunasekaran, Assistant Professor, Zoology department, Bharathiar University, Coimbatore. No human subjects were used in the study, ensuring that human ethical considerations were not applicable.

References

1. Swapnil A, Zini C, Dishant Kumar M, Renu G, Cheta S, Surbhi J. The Real Burden of Tuberculosis Hidden Cases Diagnosed on Autopsy at a Tertiary Care Center of India. Int. J. Mycobact. 2022;11(1):47-50. https://doi.org/10.4103/ijmy.ijmy_227_21
2. Pandian NSG, Sankar H, Ramalingam S, Saravana R. Hepatoprotective Effect of Hydroalcoholic Extract of *Vitis vinifera* L Seed on Paracetamol-Induced Liver Damage in Albino Rats. Trop. J Nat. Prod. Res. 2024;8(2):6261-6266. http://www.doi.org/ 10.26538/tjnpr/v8i2.25
3. John Sylvester Nas B, Corrinnette Panaga L, Mikaela Florendo G, Daves Gacutan T, Alyanna Celine Dator V, Mary Ann Cesario G, Rina Andrea Delos Santos R, James Patrick Mendez P, Mariel Jose C, Eliana Rachelle Tamana C. *in silico* Characterization of Toxicophores Found in Lemongrass (*Cymbopogon citratus*) and its Molecular Interaction with Kidney and Liver Enzymes. J. Prev. Diagn. Treat. Strateg. Med. 2023;2(2):119-128. https://doi.org/10.4103/jpdtsm.jpdtsm_71_23
4. Sheidu AR, Umar ZA, Abubakar A, Ahmed CB, Garba MM, Ogere AI, Murtala SO. Antioxidant and Hepatoprotective Potentials of Methanol Extract of *Ficus platyphylla* Stem Bark Delile (Moraceae) in Wistar Rats. Trop. J Nat. Prod. Res. 2020;4(3):91-97. https://doi.org/10.26538/tjnpr/v4i3.6
5. Fathy M, Darwish MA, Abdelhamid ASM, Alrashedy GM, Othman OA, Naseem M, Dandekar T, Othman EM. Kinetin Ameliorates Cisplatin-Induced Hepatotoxicity and

Lymphotoxicity *via* Attenuating Oxidative Damage, Cell Apoptosis and Inflammation in Rats. Biomedicines. 2022;10(7):1620. https://doi.org/10.3390/biomedicines1007 1620
6. Gohtama S, Raphaella, Ginting NC, Chiuman L. Protective Effects of *Glycine max* (L.) Merr. Ethanol Extract against Acetaminophen-Induced Nephrotoxicity and Hepatotoxicity in Wistar Rats. Trop. J Nat. Prod. Res. 2024;9(1):404 –410 https://doi.org/10.26538/tjnpr/v9i1.51
7. Iqbal MO, Yahya EB, Andleeb S, Ahmed MM, Javaid MU, Shakeel W, Iqbal I. *in vivo* assessment of reversing Cisplatin-Induced nephrotoxicity using *Jatropha mollissima* crude extract and its potential cytotoxicity. Saudi J. Biol. Sci. 2021; 28(12): 7373-7378. https://doi.org/10.1016/j.sjbs.2021.08.057
8. Zong Y, Li H, Liao P, Chen L, Pan Y, Zheng Y, Zhang C, Liu D, Zheng M, Gao J. Mitochondrial dysfunction: mechanisms and advances in therapy. Sig. Transduct Target Ther. 2024;9:124. https://doi.org/10.1038/s41392-024-01839-8
9. Soleimani V, Delghandi PS, Moallem SA, Karimi G. Safety and toxicity of silymarin, the major constituent of milk thistle extract: an updated review. Phyther. Res. 2019;33(6):1627-1638.
10. Al-Kadi A, Ahmed AS, El-Tahawy NFG, Khalifa MMA, El-Daly M. Silymarin protects against sepsis-induced acute liver and kidney injury *via* anti-inflammatory and antioxidant mechanisms in the rat. J. Adv. Biomed. Pharm. Sci. 2020;3(4):190-197.
11. Ghzaiel I, Zarrouk A, Nury T, Libergoli M, Florio F, Hammouda S, Menetrier F, Avoscan L, Yammine A, Samadi M, Latruffe N, Biressi S, Levy D, Paulo Bydlowski S, Hammami S, Vejux A, Hammami M, Lizard G. Antioxidant Properties and Cytoprotective Effect of *Pistacia lentiscus* L. Seed Oil against 7β-Hydroxycholesterol-Induced Toxicity in C2C12 Myoblasts: Reduction in Oxidative Stress, Mitochondrial and Peroxisomal Dysfunctions and Attenuation of Cell Death. Antioxidants. 2021;10:1772. https://doi.org/10.3390/antiox10111772
12. Petrovic S, Arsic A, Ristic-Medic D, Cvetkovic Z, Vucic V. Lipid Peroxidation and Antioxidant Supplementation in Neurodegenerative Diseases: A Review of Human Studies. Antioxidants. 2020;9(11):1128. https://doi.org/10.3390/antiox9111128
13. Curcio A, Romano A, Cuozzo S, Di Nicola A, Grassi O, Schiaroli D, Nocera GF, Pironti M. Silymarin in combination with vitamin C, Vitamin E, coenzyme Q10, and selenomethionine to improve liver enzymes and blood lipid profile in NAFLD patients. Medicina. 2020;56(10):544. https://doi.org/10.3390/medicina56100544
14. Gillessen A, Schmidt HHJ. Silymarin as Supportive Treatment in Liver Diseases: A Narrative Review. Adv Ther. 2020;37:1279–1301. https://doi.org/10.1007/ s12325-020-01251-y
15. Madiha Jaffar H, Al-Asmari F, Atta Khan F, Abdul Rahim M, Zongo E. Silymarin: Unveiling its pharmacological spectrum and therapeutic potential in liver diseases—A comprehensive narrative review. Food Sci. Nutr. 2024;12:3097–3111. https://doi.org/10.1002/fsn3.4010
16. Wang Y, Yuan AJ, Wu YJ, Wu LM, Zhang L. Silymarin in cancer therapy: Mechanisms of action, protective roles in chemotherapy-induced toxicity, and nanoformulations. J. Func. Foods. 2023;100:105384. https://doi.org/10.1016/j.jff.2022.105384
17. Hosseinabadi T, Lorigooini Z, Tabarzad M, Salehi B, Rodrigues CF, Martins N, Sharifi-Rad J. Silymarin antiproliferative and apoptotic effects: Insights into its clinical impact in various types of cancer. Phyther. Res. 2019;33(11):2849-2861. https://doi.org/10.1002/ptr.6470
18. Dogan D, Meydan I, Komuroglu AU. Protective Effect of Silymarin and Gallic Acid against Cisplatin-Induced Nephrotoxicity and Hepatotoxicity. Int. J. Clin. Pract. 2022; 6541026. https://doi.org/10.1155/2022/6541026
19. Yang W, Liang Z, Wen C, Jiang X, Wang L. Silymarin Protects against Acute Liver Injury Induced by Acetaminophen by Downregulating the Expression and Activity of the CYP2E1 Enzyme. Molecules. 2022;27(24):8855. https://doi.org/10.3390/molecules27248855
20. Fitrya F, Elfita E, Kurniawaty NF, Ahsan AN, Amriani A, Agustiarini V, Novita RP. Hepatoprotective effect of ethanol extract of Chinese betel herb (*Peperomia pellucida* (L.)) on CCl_4-induced hepatotoxicity in experimental animals. Trop J Nat Prod Res. 2025;9(7):3092 –3096 https://doi.org/10.26538/tjnpr/v9i7.21
21. Lalita Ambigai S, Virusha N, Geetha S. Antibacterial effects of *Musa* sp. ethanolic leaf extracts against methicillin – resistant and susceptible *Staphylococcus aureus*. S. Afr. J. Chem. Eng. 2021; 35:107 – 110. https://doi.org/10.1016/j.sajce.2020.09.007
22. Ujowundu FN, Kalu JO, Ujowundu CO, Onyeocha IO, Onuoha CH, Ibeh RC, Obasi UK, Ntaji OE, Chigbu IF, Ezirim CY. Investigating the Effect of Flavonoid, Saponin, Alkaloids, and Tannins Extracted from *Combretum dolichopentalum* Diels in CCl_4-Induced Hepatotoxicity. Trop. J Nat. Prod. Res. 2022;6(8):1255-1261. https://doi.org/doi.org/10.26538/tjnpr/v6i8.16
23. Michael HSR, Mohammed NB, Ponnusamy S, Edward Gnanaraj W. A Folk Medicine: *Passiflora incarnata* L. Phytochemical Profile with Antioxidant Potency. Turk. J Pharm. Sci. 2022;19(3):287-292. http://www.doi.org/10.4274/tjps.galenos.2021.88886
24. Anguraj A, Helan Soundra Rani M, Sathish S, Gogul Ramnath M, Rathish Kumar S. A comparative study on biosynthesized silver nanoparticles from *H. undatus* fruit peel and their therapeutic applications. Discover Nano. 2024;19:49. https://doi.org/ 10.1186/s11671-024-03995-w
25. Sachin K Singh, Pavankumar C, Vinoth K, Chaitanya M, Rashmi SP, Saranya P, Sukriti V, Avijit M, Prathiba P, Smriti A, Amandeep S, Navneet K, Patrick A, Yogendra P, Vetriselvan S, Wong LS, Gaurav G, Mohamed M. Abdel-Daim, Jon A, Kamal D. Unravelling the nutraceutical and therapeutic perspectives of corosolic acid: Journey so far and the road ahead. Phytochemistry Reviews. 2025. https://doi.org/ 10.1007/s11101-025-10146-1.
26. Abdulhafiz F, Reduan MFH, Hisam AH, Mohammad I, Abdul Wahab IR, Abdul Hamid FF, Mohammed A, Nordin ML, Shaari R, Bakar LA, Kari ZA, Wei LS, Goh KW, Ahmad Mohd Zain MR. LC–TOF-MS/MS and GC-MS based phytochemical profiling and evaluation of wound healing activity of *Oroxylum Indicum* (L.) Kurz (Beka). Front. Pharmacol. 2022;13:1050453. https://doi.org/10.3389/fphar.2022.105045
27. Khazaei R, Seidavi A, Bouyeh M. A review on the mechanisms of the effect of silymarin in milk thistle (*Silybum marianum*) on some laboratory animals. Vet. Med. Sci. 2022;8:289–301. https://doi.org/10.1002/vms3.641
28. Chinedu E, Samuel Ehiabhi O. Ethnomedicinal, Phytochemical, and Pharmacological Review of Asclepiadaceae. J. Prev. Diagn. Treat. Strategies Med. 2023;2(1):03-18. https://doi.org/10.4103/jpdtsm jpdtsm_100_22
29. Qian A, Zhou L, Shi D, Pang Z, Lu B. *Portulaca oleracea* alleviates CCl4-induced acute liver injury by regulating hepatic S100A8 and S100A9. Chin. Herb. Med. 2022;15(1):110-116. https://doi.org/10.1016/j.chmed.2022.05.004
30. Dugawale TP, Khanwelkar CC, Durgawale PP. Primary Phytochemical Evaluation of *P. oleracea* and *P. quadrifida*. Res. J Pharm. Technol. 2021;14(7):3789-3793. https://doi.org/10.52711/0974-360X.2021.00656
31. Syed Kamil M, Liyakha T, Ahmed MD, Paramjyothi S. Neuropharmacological Effects of Ethanolic Extract of *Portulaca quadrifida* Linn. In Mice. Int. J. Pharm. Res. 2020; 2:1386-1390.
32. Liang J, Zhao G, Bian Y, Bi G, Sui Q, Zhang H, Shi H, Shan G, Huang Y, Chen Z, Wang L, Zhan C. HNF4G increases cisplatin resistance in lung adenocarcinoma *via* the MAPK6/Akt pathway. PeerJ. 2023;11:14996. https://doi.org/ 10.7717/peerj.14996
33. Ghorani V, Saadat S, Khazdair MR, Gholamnezhad Z, El-Seedi H, Boskabady MH. Phytochemical Characteristics and Anti-Inflammatory, Immunoregulatory, and Antioxidant Effects of

Portulaca oleracea L.: A Comprehensive Review. Evid. Based Complement Alternat. Med. 2023;2023:29. https://doi.org/10.1155/2023/2075444
34. Chen JY, Tsai CL, Tseng CY, Yu PR, Chang YH, Wong YC, Lin HH, Chen JH. *in vitro* and *in vivo* Nephroprotective Effects of *Nelumbo nucifera* Seedpod Extract against Cisplatin-Induced Renal Injury. Plants. 2022;11(23):3357. https://doi.org/10.3390/plants11233357
35. Shomer NH, Allen-Worthington KH, Hickman DL, Jonnalagadda M, Newsome JT, Slate AR, Valentine H, Williams AM, Wilkinson M. Review of Rodent Euthanasia Methods. J. Am. Assoc. Lab. Anim. Sci. 2020;59(3):242-253. http://dx.doi.org/ 10.30802/AALAS-JAALAS-19-000084
36. Sinaga E, Fitrayadi A, Asrori A, Rahayu SE, Suprihatin S, Prasasty VD. Hepatoprotective effect of *Pandanus odoratissimus* seed extracts on paracetamol-induced rats. Pharma. Bio. 2021;59(1):31-39. https://doi.org/10.1080/13880209 .2020.1865408
37. Lala V, Zubair M, Minter DA. Liver Function Tests. In: StatPearls. Treasure Island (FL): StatPearls Publishing, 2024. https://www.ncbi.nlm.nih.gov/books/NBK482489/
38. Hassan OY, Khatal AA, Alagouri II, Eljrieby LR, Aljaghdaf HM, Muftah SS. Study of the Histological and Histopathological Effects of Garlic Extract (*Allium sativum*) on Cisplatin-Induced Kidney Damage in Rabbits. J. Advan. Medi. Medi. Res. 2023;35(22):134-152. https://doi.org/10.9734/jammr/2023/v35i225255
39. Aguilar Diaz De Leon J, Borges CR. Evaluation of Oxidative Stress in Biological Samples Using the Thiobarbituric Acid Reactive Substances Assay. J. Vis. Exp. 2020;159. https://doi.org/10.3791/61122
40. N'Guessan MF, Sery BB, Vanie FJ, Ekissi NA, Djohan YF, Coulibaly FA, Djaman AJ. Evaluation of Glutathione Peroxidase Enzymatic Activity in Seminal Plasma of Patients Treated at the Institute Pasteur in Cote d'Ivoire. Adv. in Reprod. Sci. 2023;11:116-126. https://doi.org/10.4236/arsci.2023.114011
41. Murphy MP, Bayir H, Belousov V, Chang CJ, Davies KJA, Davies MJ, Dick, TP, Finkel T, Forman HJ, Janssen-Heininger Y, Gems D, Kagan VE, Kalyanaraman B, Larsson, NG, Milne GL, Nystrom T, Poulsen HE, Radi R, Remmen HV, Schumacker PT, Thornalley PJ, Toyokuni S, Winterbourn CC, Yin H, Halliwell B. Guidelines for measuring reactive oxygen species and oxidative damage in cells and *in vivo*. Nat Metab. 2022;4:651–662. https://doi.org/10.1038/ s42255-022-00591-z
42. Makiyah SNN, Usman S, Dwijayanti DR. *in silico* Toxicity Prediction of Bioactive Compounds of *Dioscorea alata* L. Trop. J Nat. Prod. Res. 2022;6(10):1587-1596. http://www.doi.org/10.26538/tjnpr/v6i10.5
43. Volkov V, Lobanov A, Voronkov M, Baygildiev T, Misin V, Tsivileva O. Kinetics and Mechanism of Epinephrine Autoxidation in the Presence of Plant Superoxide Inhibitors: A New Look at the Methodology of Using a Model System in Biological and Chemical Research. Antioxidants. 2023;12(8):1530. https://doi.org/10.3390/ antiox12081530
44. Jaganjac M, Sredoja Tisma V, Zarkovic N. Short Overview of Some Assays for the Measurement of Antioxidant Activity of Natural Products and Their Relevance in Dermatology. Molecules. 2021;26(17):5301. https://doi.org/10.3390/ molecules 26175301
45. Murugesan V, Palanivel P, Ramesh G, Ganesh D, Michael HSR, Bandhumy Lingam S, Sivaraman RK. Exploring the antibacterial potential of *Clidemia hirta* leaf extract against the pathogenicity of *Pseudomonas aeruginosa: in vitro* and *in silico* approaches. Front. Pharmacol. 2025;16:1555542. https://doi.org/10.3389/fphar. 2025.1555542
46. Chakravorty A, Hussain A, Cervantes LF, Lai TT, Charles L. Exploring the Limits of the Generalized CHARMM and AMBER Force Fields through Predictions of Hydration Free Energy of Small Molecules. Brooks III. J. Chem. Inf. Model. 2024;64(10):4089-4101. https://doi.org/10.1021b/ acs.jcim.4c 00126
47. Jawahar Nuziba Begum A, Govindaraj M, Murugasamy Maheswari K, Raamji S, Sivaraman RK, Michael HSR, Chandramohan V, Rathnasamy S, Bandhumy Lingam S. *in silico* docking and dynamics of selected secondary metabolites of *Albizia lebbeck* against Androgen Receptor (AR) for the treatment of prostate cancer. J. Microbiol. Biotechnol. Food Sci. 2024;14(3):10608. https://doi.org/10.55251/jmbfs.10608
48. Sinaga E, Fitrayadi A, Asrori A, Rahayu SE, Suprihatin S, Prasasty VD. Hepatoprotective effect of *Pandanus odoratissimus* seed extracts on paracetamol-induced rats. Pharm Biol. 2021;59(1):31-39. https://doi.org/10.1080/13880209.2020.1865408
49. Ghorani V, Saadat S, Khazdair MR, Gholamnezhad Z, El-Seedi H, Boskabady MH. Phytochemical Characteristics and Anti-Inflammatory, Immunoregulatory, and Antioxidant Effects of *Portulaca oleracea* L.: A Comprehensive Review. Evid Based Complement Alternat Med. 2023; 2023:2075444. https://doi.org/10.1155/2023/ 2075444
50. Farkhondeh T, Samarghandian S. The therapeutic effects of *Portulaca oleracea* L. in Hepatogastric disorders. Gastroenterología y Hepatología. 2019;42(2):127-132. https://doi.org/10.1016/j.gastrohep.2018.07.016
51. Sudhakar D, Krishna Kishore R, Parthasarathy PR. *Portulaca oleracea* L. extract ameliorates the cisplatin-induced toxicity in chick embryonic liver. Indian J Biochem Biophys. 2010;47(3):185-9.
52. **Karplus M, McCammon JA. Molecular dynamics simulations of biomolecules. Nat Struct Biol. 2002;9(9):646-652** https://doi.org/10.1038/nsb0902-646
53. **Hollingsworth SA, Dror RO. Molecular Dynamics Simulation for All. Neuron. 2018;99(6):1129-1143** https://doi.org/10.1016/j.neuron.2018.08.011
54. Moritsugu K, Terada T, Kidera A. Free-Energy Landscape of Protein-Ligand Interactions Coupled with Protein Structural Changes. *J Phys Chem B.* 2017;121(4):731-740 https://doi.org/10.1021/acs.jpcb.6b11696
55. Kollman PA, Massova I, Reyes C, et al. Calculating structures and free energies of complex molecules: combining molecular mechanics and continuum models. *Acc Chem Res*. 2000;33(12):889-897 https://doi.org/10.1021/ar000033j
56. Genheden S, Ryde U. The MM/PBSA and MM/GBSA methods to estimate ligand-binding affinities. *Expert Opin Drug Discov*. 2015;10(5):449-461 https://doi.org/10.1517/17460441.2015.1032936